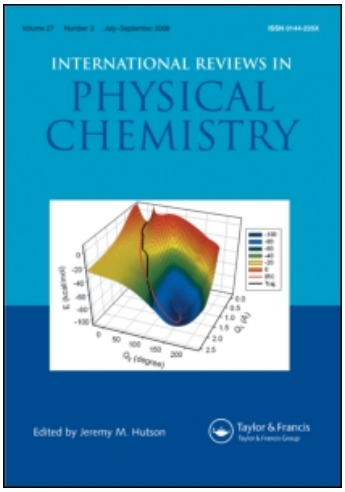

International Reviews in Physical Chemistry
Publication details, including instructions for authors and subscription information:
http://www.informaworld.com/smpp/title~content=t713724383

Natural bond orbital analysis of the intrinsic reaction barriers in nucleophilic displacements

Ikchoon Lee[a]
[a] Department of Chemistry, Inha University, Inchon, South Korea

Online publication date: 26 November 2010

To cite this Article Lee, Ikchoon(2003) 'Natural bond orbital analysis of the intrinsic reaction barriers in nucleophilic displacements', International Reviews in Physical Chemistry, 22: 2, 263 — 283
To link to this Article: DOI: 10.1080/0144235031000086058
URL: http://dx.doi.org/10.1080/0144235031000086058

INT. REVIEWS IN PHYSICAL CHEMISTRY, 2003
VOL. 22, NO. 2, 263–283

Taylor & Francis
Taylor & Francis Group

Natural bond orbital analysis of the intrinsic reaction barriers in nucleophilic displacements

IKCHOON LEE†
Department of Chemistry, Inha University, Inchon 402-751, South Korea

Applications of natural bond orbital (NBO) analysis to the intrinsic reaction barriers involved in identity nucleophilic substitutions of halides (X = F, Cl or Br) at various carbon centres such as methyl, acyl, vinyl, imidoyl, cyclopropenyl and cyclopentadienyl halides are surveyed. The most important transition state stabilization in the π attack ($S_N\pi$) path is the proximate $\sigma \rightarrow \sigma^*$ charge-transfer interactions, while that in the σ attack ($S_N\sigma$) path is the non-charge-transfer term which includes bond energy, exclusion repulsion and electrostatic interactions. The tighter transition state with shorter C–X bond distance coupled with stronger bond energy for X = F often provides additional stabilization owing to stronger energy gain. In the open (loose) $S_N\sigma$ transition state, the leaving group X^- leaves behind an empty p (p^+) orbital at C_α, which leads to strong $\pi_{C=C} \rightarrow p^+$ and/or $n_X \rightarrow p^+$ charge-transfer stabilization. In the $S_N\pi$ transition state the major stabilizing factors are $n \rightarrow \sigma^*_{C-X}$ and/or $\pi_{C=C} \rightarrow \sigma^*_{C-X}$ type charge-transfer interactions. The NBO analysis is shown to provide satisfactory explanations of the origins of intrinsic reaction barriers based on orbital interaction concepts.

Contents

† Email: ilee@inha.ac.kr

International Reviews in Physical Chemistry ISSN 0144–235X print/ISSN 1366–591X online © 2003 Taylor & Francis Ltd
http://www.tandf.co.uk/journals
DOI: 10.1080/0144235031000086058

1. Introduction

Nucleophilic displacement at saturated carbon is one of the most important reaction in both synthetic and mechanistic organic chemistry. Studies of bimolecular nucleophilic substitution reactions in the gas phase have been particularly valuable as they allow investigation of various intrinsic molecular reactivity factors without involvement of solvent. The most thoroughly studied reactions are the gas-phase identity methyl transfer reactions involving halide anions [1–3], $R = CH_3$ with $X = F$, Cl, Br and I in the following equation, especially with $X = Cl$:

$$X^- + RX \rightarrow XR + X^-. \quad (1)$$

Ab initio molecular orbital calculations have also been extended to the gas-phase identity nucleophilic substitution reactions at various primary and secondary carbons [1*g*], at various acyl functional centres [4] and at vinylic [5] and other unsaturated carbon centres [6–8] in order to determine mechanisms and intrinsic reactivities of substitution involving various reaction centres.

For the general thermoneutral concerted gas-phase nucleophilic displacement reaction given by equation (1), the activation barrier is a measure of the intrinsic reactivity of a nucleophile X^- toward a reaction centre R in the absence of both solvent effects and thermodynamic driving force. Thus intrinsic barriers have been determined quantitatively for some nucleophiles at various reaction centres, by both theoretical [1(*g*, *h*), 4–8] and experimental techniques [3*a*, 9–11].

It is, however, essential to understand the origins of the barrier to conceptualize reactivity patterns. In other words in order to comprehend and explain the mechanism and reactivity of a reaction involving certain reactants, e.g. RX and X^-, it is important to analyse and understand factors that cause the reaction barrier of the reaction to form. In this review, we present analyses of such intrinsic reaction barriers involved in the identity halide exchanges, equation (1) with $X = F$, Cl and Br, based on the natural bond orbital (NBO) method [12–14].

Pross and co-workers [1*a*, 15] proposed a model to explain reactivity trends based on curve crossing diagrams. They described the formation of the barrier, thereby enabling complex reactivity patterns in a variety of chemical reaction to be comprehended by the use of valence bond (VB) configurations which are based either on fragment orbitals (the state correlation diagram (SCD) model) or on atomic orbitals (the VB configuration mixing model). Their model, although useful with a wide range of applicability, lacks quantitative accuracy in predicting reactivities, most probably because electron correlation effects are improperly accounted for. For example, their SCD model predicts the relative reactivity of halide anions in the gas-phase identity methyl transfer reactions as $F^- < Cl^- < Br^-$, which is in agreement with that predicted at the uncorrelated RHF/4-31G [1(*a*), 16)] (and RHF/6-311++G(3df,2p) [1(*n*)]) level of theory but is not consistent with the reactivity trend predicted by the high level correlated MO (G2(+)) calculations of $Cl^- < Br^- < F^-$ [1(*n*)]. The lowest reactivity of F^- predicted by the SCD (and uncorrelated molecular orbital (MO) (4-31G) calculation) is in fact the greatest reactivity among the three halide nucleophiles. Thus the curve crossing model leaves much to be desired in proper accounting of the electron correlation effects.

In the following we introduce an alternative way of analysing the intrinsic reaction barriers based on the NBO theory developed by Weinhold and co-workers [12–14]. In NBO analysis, the input basis set is transformed successively into various localized basis sets, first to natural atomic orbitals and then to hybrid orbitals (such

as h_A, h_B, etc.), which are used to form bond orbitals (NBOs). Between atoms A and B a localized σ bond σ_{AB} and an antibond σ^*_{AB} are formed:

$$\sigma_{AB} = c_A h_A + c_B h_B; \tag{2a}$$

$$\sigma^*_{AB} = c_B h_A - c_A h_B. \tag{2b}$$

Finally the NBOs are transformed into localized MOs. Here the symbol σ represents all types of filled (core (c), lone pair (n), σ and π, etc.) orbitals and σ^* represents all types of unfilled (σ^*, π^*) and extra-valence shell Rydberg (r) orbitals. In the NBO basis, the density matrix is partitioned into two blocks, a block ($\Gamma_{\sigma\sigma}$) associated with the highly occupied NBOs of the natural Lewis structure and a block ($\Gamma_{\sigma^*\sigma^*}$) associated with the remaining weakly occupied NBOs of antibond and Rydberg type. The off-diagonal matrix elements connecting these two blocks ($\Gamma_{\sigma\sigma^*}$) represent the $\sigma \rightarrow \sigma^*$ mixing of filled and unfilled orbitals. These interactions give the weak departures from a strictly localized natural Lewis structure that constitute the primary 'non-covalent' effects. The $\sigma \rightarrow \sigma^*$ interaction results in second-order energy lowering, $\Delta E^{(2)}_{\sigma\sigma^*}$ in the following equation [13, 17], and corresponding geometry changes associated with the Fock matrix element $F_{\sigma\sigma^*}$:

$$\Delta E^{(2)}_{\sigma\sigma^*} = -2\frac{F^2_{\sigma\sigma^*}}{\varepsilon_{\sigma^*} - \varepsilon_{\sigma}}. \tag{3}$$

Formally, the $\sigma_{AB} \rightarrow \sigma^*_{CB}$ NBO charge-transfer (CT) interaction leads to an equal decrease in A–B and C–D bond orders (bond stretching) and a simultaneous increase in B–C bond order (bond contraction) [13, 14]. Thus the localized MO, Ψ^{LMO}_{AB}, associated with a localized bond A–B may be written in NBO form as

$$\Psi^{LMO}_{AB} \cong \sigma_{AB} + \delta\sigma^*_{CD} + \cdots, \tag{4}$$

where the small contribution (δ) of the antibond σ^*_{CD} is the irreducible delocalization of σ_{AB} from an idealized localized form due to non-covalent CT interactions. This type of $\sigma \rightarrow \sigma^*$ mixing is particularly efficient between two proximate (geminal and vicinal) bonds leading to CT (delocalization) stabilization. A notable example of an *intra*molecular vicinal $\sigma_{CH} \rightarrow \sigma^*_{CH}$ CT stabilization effect is that found with the enhanced energy lowering in the staggered form of ethane compared with the eclipsed form. In the staggered form the two σ and σ^* bonds are oriented in an antiperiplanar fashion rendering more effective CT-energy lowering than in the eclipsed form where the two bonds are synperiplanar [12]. The origin of the rotational barrier in ethane rests therefore mainly in the difference in the vicinal charge transfer stabilization energies rather than in the repulsive steric and electrostatic energy differences between the two forms [12].

When two molecules approach and form an adduct, which can be a stable intermediate, a transition state or a simple complex such as a hydrogen-bonded water dimer, the adduct formation energy can be decomposed into CT and non-charge-transfer (NCT) parts [13]:

$$\begin{aligned}\Delta E &= E(\text{adduct}) - E(\text{isolated molecules}) \\ &= \Delta E_{NCT} + \Delta E_{CT}.\end{aligned} \tag{5}$$

The total CT energy, ΔE_{CT}, can be estimated by deleting Fock matrix elements $F_{\sigma\sigma^*}$ and determining the change in the total energy. In addition one can follow a complete picture of a specific $\sigma \rightarrow \sigma^*$ interaction, ranging from its quantitative

numerical value or effect on the optimized molecular geometry to its qualitative origin in the shape or diffuseness of the associated orbitals.

The remaining part of the binding energy, ΔE_{NCT} in equation (5), is due to exclusion repulsion (steric) and electrostatic (induction and polarization) multipole effects associated with the charge distributions of isolated molecules. A well-established example of the *inter*molecular NBO analysis is that of hydrogen bonding in the water dimer [13, 18]. The n_o–σ^*_{CH} CT interaction along the H bond axis was found to play a critical role in the formation of the hydrogen bond, and these interactions provide stabilization energy of 3–5 kcal mol^{-1} at the observed equilibrium distance.

The NBO analysis can illuminate interesting chemical aspects of the bonding and allow explanations of the various intra- and intermolecular energy barriers based on orbital interaction concepts. In the following we present applications of the NBO analysis to comprehend the origins of the intrinsic barriers involved in the gas-phase nucleophilic substitution reactions.

2. Methyl transfer reactions

Methyl transfer reactions have long provided prototypes of bimolecular nucleophilic substitution (S_N2) reactions at carbon [1–3]. The gas-phase methyl transfer reactions have come under close scrutiny both experimentally [3] and theoretically [1, 2]. Of particular interest are the gas-phase identity halide exchanges, $R = CH_3$ with $X = F$, Cl, Br and I in equation (1), with special attention being focused on chloride exchange ($X = Cl$). *Ab initio* results have been reported at various levels of theory on the identity methyl transfer reaction with halides [1]. These reactions are found to proceed through a double-well potential energy profile (figure 1). Initially, a reactant (ion–molecule) complex (RC) with C_{3v} symmetry is formed with a complexation energy of ΔE_{RC}. The RC then proceeds to the product complex, which is identical to RC, through the transition state (TS) overcoming the central energy barrier ($\Delta E^{\neq}_{C}$). The activation energy relative to the reactants' level is given as $\Delta E^{\neq}$. Four types of energy changes are possible: pure electronic energy ($\Delta E^{\neq}$), zero-point energy (ZPE) corrected potential energy at 0 K ($\Delta E^{\neq}_{ZPE}$), the corrected (to 298 K) thermal energy value ($\Delta H^{\neq}$) and the free energy ($\Delta G^{\neq} = \Delta H^{\neq} - T\,\Delta S^{\neq}$). Various experimental and theoretical gas-phase activation barriers are surveyed in a recent paper [1(*n*)].

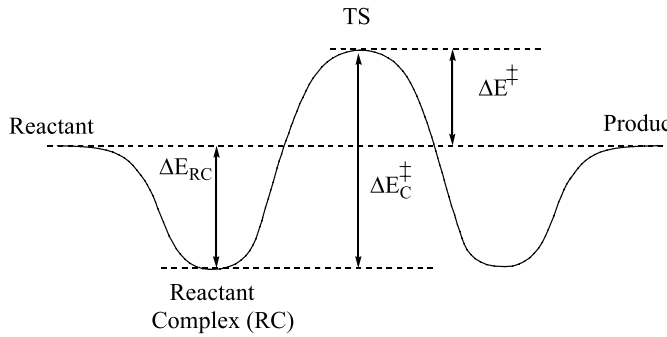

Figure 1. Double-well potential energy surface for the identity gas-phase methyl transfer reactions.

Largely because of gas-phase experimental difficulty the experimental barriers reported are very limited.

The theoretical barrier heights are sensitive to the level of electron correlation included and the size of basis sets used [1]. Table 1 summarizes some of the results reported at different levels of theory [1(*n*)]. It is notable that although the absolute values of barriers ($\Delta E^{\neq}_{ZPE}$, $\Delta H^{\neq}$ and $\Delta G^{\neq}$) differ depending on the level of accounting electron correlation (with the same basis sets) the correlated barriers increase in the general order F < Br < Cl. In contrast, however, the uncorrelated RHF barriers increase in the general order of increasing nucleophilicity and decreasing leaving ability, Br < Cl < F. This clearly demonstrates that inclusion of the electron correlation effect is important to predict correct intrinsic barriers and reactivity order of the gas-phase methyl transfer reactions of halides.

NBO analysis of these reaction barriers reveals the origins of this reactivity trend. The results in table 2 show that although the $\sigma \rightarrow \sigma^*$ proximate CT stabilization (ΔE_{CT}) is the largest with X = F, it is the electrostatic interaction (ΔE_{es}, which is a part of ΔE_{NCT} in equation (5)) that leads to the greatest reactivity (lowest barrier) for X = F. The major component of ΔE_{CT} is the $n_X \rightarrow \sigma^*_{C-X}$ interactions, which are −110.7 (X = F), −113.3 (X = Cl) and −114.2 (X = Br) kcal mol^{-1}. In general both the energy gap $\Delta\varepsilon$ ($= \varepsilon_{\sigma^*} - \varepsilon_n$) and the Fock matrix element $F_{n\sigma^*}$ in equation (3) increase in the order X = Br < Cl < F as shown in table 3 so that the difference in ΔE_{CT} becomes small [1(*n*)].

The degree of bond formation in the TS is also the greatest for X = F with the shortest distance of C···X$^-$, which will no doubt result in the greatest exclusion repulsion. Since the bond strength of the C–F bond (bond energies [20]: 116 (C—F), 81 (C—Cl), 68 (C—Br) kcal mol^{-1}) is the largest, the deformation energy [1(*a*), 21], the major component of which is the stretching of C—F, is also the largest although the actual $r^{\neq}$ is the shortest. It is noteworthy that the lower the intrinsic barrier ($\Delta E^{\neq}$), the greater is the degree of bond formation ($\Delta n^{\neq}$) [22] in the TS.

Table 1. Activation barriers (kcal mol^{-1}) for the gas-phase identity methyl transfer reactions at various levels with the 6-311++G(3df,2p) basis sets.

Method	X	$\Delta E^{\neq}_{ZPE}$	$\Delta H^{\neq}$	$\Delta G^{\neq}$
RHF	F	7.6 (14.5)[a]	6.8	15.0
	Cl	6.9 (10.9)[a]	6.4	14.0
	Br	5.1	4.8	12.2
DFT[b]	F	−4.3	−5.1	3.0
	Cl	−1.1	−1.6	6.0
	Br	−2.8	−3.2	4.3
MP2	F	0.0	−0.8	7.5
	Cl	4.8	4.2	12.0
	Br	3.1	2.7	10.4
QCISD(T)	F	−1.5	−2.3	6.0
	Cl	3.0	2.5	10.3
	Br	1.2	0.8	8.5

[a] The $\Delta E^{\neq}$ value at the 4-31G level [19].
[b] B3LYP.

Table 2. The results of NBO analysis and relevant data for the gas-phase identity methyl transfer reactions: $X^- + CH_3X \rightleftharpoons XCH_3 + X^-$ with X = F, Cl, and Br. All energies are in kcal mol^{-1}.

X	$\Delta E^{\neq a}$	$\Delta E_{CT}{}^{b}$	$\Delta E_{es}{}^{c}$	$\Delta E_{def}{}^{b,d}$	$r^{\neq}$ (Å)^{e}	$\Delta n^{\neq}$ (%)^{f}
F	−1.3	−104.9	−316.8	39.0	1.825	48.0
Cl	3.3	−81.6	−71.0	33.0	2.321	40.9
Br	1.6	−74.6	−11.4	28.5	2.479	41.1

[a] Electronic activation energies at QCISD(T)/6-311++G(3df,2p) level.
[b] Calculated at QCISD(T)/6-311++G(3df,2p) level.
[c] Electrostatic energy changes calculated using charge densities obtained at AIM-QCISD/6-311++G(3df,2p)//QCISD(T)/6-311++G(3df,2p) level.
[d] Deformation energies.
[e] The C—X bond length in the TS at QCISD(T)/6-311++G(3df,2p) level.
[f] Percentage bond order change in the TS calculated from $\Delta n^{\neq} = \{[\exp(-r^{\neq}/a) - \exp(-r_P/a)]/[\exp(-r_R/a) - \exp(-r_P/a)]\} \times 100\%$ where $r^{\neq}$, r_R and r_P are the bond length in the TS, reactant and product ($r_R = r_P$) respectively and $a = 0.6$.

3. Acyl transfer reactions

Mechanisms of nucleophilic additions to the acyl group of acid derivatives can be discussed in the context of the acyl group transfer between two nucleophiles as an acceptor and donor [23]. The term 'acyl' refers normally to the 'carbonyl' group (RCO—), but it may be used as a general term to represent any group derived from acids, e.g. thiocarbonyl (RCS—), sulphonyl (RSO_2—), sulphinyl (RSO—) and neutral phosphoryl ($(RO)_2PO$—) etc. [4(*b*)]. The gas-phase identity carbonyl transfers

$$X^- + R{-}\overset{\overset{O}{\|}}{C}{-}X \rightleftharpoons X{-}\overset{\overset{O}{\|}}{O}{-}R + X^- \qquad (6)$$

involving halides X = F, Cl, Br are known to proceed either concertedly exhibiting a double-well potential energy profile (figure 1) or stepwise through a tetrahedral intermediate (T^-) with a triple-well (or single-well) potential energy surface [4]. Normally the $\pi^*_{C=O}$ is much lower than the σ^*_{C-X} ($\Delta\varepsilon = \varepsilon_{\sigma^*} - \varepsilon_{\pi^*} \gg 0$) level [4(*b*, *c*)]. The initial attack of X^- occurs therefore on the $\pi^*_{C=O}$ orbital, which is orthogonal to the σ^*_{C-X} orbital in the reactant, RCOX, but the adduct, RXCOX, tends to form a tetrahedral (TS or intermediate) geometry where $\pi^*_{C=O}$ and σ^*_{C-X} are no longer orthogonal and mixing of the two lowest unoccupied MOs (LUMOs), $\pi^*_{C=O}$ and σ^*_{C-X}, is now possible. If the two MOs are separated by a large energy gap ($\Delta\varepsilon$ = large), the mixing effect will be small and the nucleophile forms a tetrahedral intermediate (T^-) through the π attack. When, however, the energy gap is small the $\pi^* \rightarrow \sigma^*$ orbital mixing becomes efficient and the σ^*_{C-X} MO becomes a main component of the LUMO [4(*c*), 24]. Thus the π attack of the nucleaphile induces the C—Cl bond cleavage in a concerted process. The narrower $\Delta\varepsilon$, the greater is the proclivity for a concerted acyl transfer rather than a stepwise transfer through an intermediate. The energy gap ($\Delta\varepsilon$) calculated by the NBO method with HF/6-311+G** basis set (using MP2/6-311+G** geometries) was 3.9 and 3.1 eV for HCOCl and CH_3COCl respectively [4(*c*)]. For X = Br, they were even smaller: 1.5 and 0.6 eV. These $\Delta\varepsilon$ values are much smaller than those with X = F, 7.8 and 7.0 eV

Table 3. Major vicinal CT interactions in the trigonal bipyramidal pentacoordinate (TBP-5C) transition states for methyl transfer reactions $X^- + CH_3X \rightleftharpoons XCH_3 + X^-$.

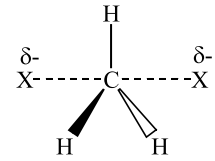

D_{3h} (TBP-5C) TS

X^-	Interaction[a]	$\Delta\varepsilon = \varepsilon_{\sigma^*} - \varepsilon_{\pi^*}$ (a.u)	$F_n\sigma^*$ (a.u)	$-\Delta E^{(2)\,b}_{n\sigma^*}$ (kcal mol^{-1})
F	$n_F \rightarrow \sigma^*_{C-H}$	1.32	0.08	18.2 (3×)[c]
	$n_F \rightarrow \sigma^*_{C-F}$	1.55	0.12	12.1
	$n_F \rightarrow \sigma^*_{C-F}$	0.86	0.26	98.6
Cl	$n_{Cl} \rightarrow \sigma^*_{C-H}$	1.07	0.05	7.5 (3×)
	$n_{Cl} \rightarrow \sigma^*_{C-Cl}$	1.14	0.08	7.6
	$n_{Cl} \rightarrow \sigma^*_{C-Cl}$	0.51	0.20	105.7
Br	$n_{Br} \rightarrow \sigma^*_{C-H}$	1.04	0.04	5.1 (3×)
	$n_{Br} \rightarrow \sigma^*_{C-Br}$	1.07	0.08	7.0
	$n_{Br} \rightarrow \sigma^*_{C-Br}$	0.44	0.19	107.2

[a] The n_X in the first two $n \rightarrow \sigma^*$ interactions is an sp^2 type while that in the third is a p type which is at higher level.
[b] Calculated from equation (3).
[c] There are three identical $n \rightarrow \sigma^*_{C-H}$ interactions and the value given is for the three interactions.

Table 4. MO levels (at RHF/6-31 + G*//B3LYP/6-31 + G* level) in a.u. and energetics in kcal mol^{-1} for carbonyl (RCOCl) and thiocarbonyl (RCSCl) transfer reactions at the B3LYP/6-311 + G(3df,2p)//B3LPY/6-31 + G* level.

Acyl type	R	ε_{π^*}	ε^*_σ	$\Delta\varepsilon^a$	ΔE
RCOCl	MeO	+0.143	+0.238	0.095	3.1 (TS)
	Me	+0.105	+0.221	0.116	−5.1 (TS)
	H	+0.079	+0.235	0.156	−10.2 (TS)
	CN	+0.021	+0.219	0.198	−20.7 (intermediate)
RCSCl	MeO	+0.061	+0.219	0.158	4.6 (TS)
	Me	+0.034	+0.208	0.174	−3.9 (TS)
	H	+0.023	+0.209	0.186	−9.3 (intermediate)
	CN	−0.030	+0.188	0.218	−17.7 (intermediate)

[a] $\Delta\varepsilon = \varepsilon_{\sigma^*} - \varepsilon^*_\pi$.

respectively, which are believed to react by a stepwise mechanism [4]. On account of the small $\Delta\varepsilon$ values, the identity gas-phase acyl transfer reactions with X = Cl and Br are much more likely to proceed concertedly through a tetrahedral TS. An electron donor R (R = MeO) raises $\pi^*_{C=O}$ more than σ^*_{C-X} (table 4) so that $\Delta\varepsilon$ becomes smaller and the reactions tends to be more likely to proceed concertedly [4(*c*)]. Conversely, an electron acceptor R (R = CN) tends to lead to a stepwise process.

Table 5. The NBO analysis[a] of proximate CT energies (ΔE_{CT}) and electrostatic energies (ΔE_{es}) in the π and σ adduct formation of $X^- + RCOX \rightleftharpoons RCOX + X^-$ (in kcal mol^{-1}).

R	X	Adduct	Symmetry	ΔE_{CT}	ΔE_{es}	ΔE^b
H	Cl	π	C_1	−212	14	−9.6
		σ	C_{2V}	32	−70	8.2
	Br	π	C_1	−259	18	−8.6
		σ	C_{2v}	41	−96	4.3
Me	Cl	π	C_1	−221	20	−7.9
	Br	π	C_1	−293	19	−6.8

[a] At the HF/6-311 + G*//MP2/6-311 + G** level.
[b] At the MP2/6-311 + G** level.

However, elevation of $\pi^*_{C=O}$ results in a smaller CT stabilization, $\Delta E^{(2)}_{\sigma-\sigma^*}$ in equation (3), so that reactivity decreases (barrier becomes higher). The examples are presented in table 4. Two types of initial approaches, σ and π, lead to two types of adduct (TS) formation. The proximate CT interactions, ΔE_{CT}, in the TS (table 5) favour the π attack over the σ attack process. The electrostatic energies ΔE_{es} are destabilizing for the π adduct, but the difference between X = Cl and Br is small [4(*c*)]. Overall, the CT stabilizations (ΔE_{CT}) are larger in the π adduct than in the σ adduct, whereas the electrostatic energies (ΔE_{es}) favour the σ adduct, albeit the stability provided is much less than that by ΔE_{CT} in the π adduct [4(*c*)]. The reactivity of X = Cl by the π attack process is greater than that of X = Br although the proximate CT stabilization energy, ΔE_{CT}, is larger with X = Br than X = Cl. This means that the NCT term, ΔE_{NCT} in equation (5), is more favourable for X = Cl. Since this term, ΔE_{NCT}, is associated with the localized HF wavefunction corresponding essentially to a Lewis structure, ΔE_{NCT} includes the bond energy (BE) of the C—X bonds in the TS. The TS structures in the π attack processes show that the TS with X = Cl is tighter with a greater degree of bond formation (61%) than that with X = Br (58%) so that a stronger BE (81 kcal mol^{-1} for C—Cl) contributes more to the π attack TS with X = Cl than that (68 kcal mol^{-1} for C—Br) with X = Br [4(*c*)].

Reference to table 4 reveals that the $\pi^*_{C=S}$ level in the thiocarbonyl group is much lower than the corresponding $\pi^*_{C=O}$ level in the carbonyl group with little energy difference between σ* levels. Thus the energy gap $\Delta\varepsilon$ ($= \varepsilon_{\sigma^*} - \varepsilon_{\pi^*}$) becomes much wider and leads to a greater proclivity for a stepwise mechanism through an intermediate [4(*c*)]. In all cases the carbonyl transfer has a somewhat lower activation barrier and a more stable intermediate than the corresponding thiocarbonyl transfers (table 4). This results from a greater degree of $\pi^* \rightarrow \sigma^*$ mixing in the carbonyl transfer TS than in the thiocarbonyl transfer TS due to the narrower energy gap ($\Delta\varepsilon$) between the two LUMOs as discussed above.

The NBO analysis indicated that the proximate $\sigma \rightarrow \sigma^*$ CT stabilization is greater in the carbonyl than in the thiocarbonyl transfers, whereas the electrostatic interactions are more *de*stabilizing in the thiocarbonyl than carbonyl transfers [4(*c*)]. This suggests that in the carbonyl transfers CT delocalization is the predominant TS stabilizing factor, but in the thiocarbonyl transfer the electrostatic interaction is the major *de*stabilizing factor, which is due to strong polarization of the thiocarbonyl group (C^+—S^-) in the TS providing strong repulsive interactions between the three negative charge centres, the two Cl^- and S^- [4(*c*)].

The transfer of neutral phosphoryl groups between basic nucleophiles can proceed concertedly [25] as well as stepwise through a TBP-5C intermediate [26]:

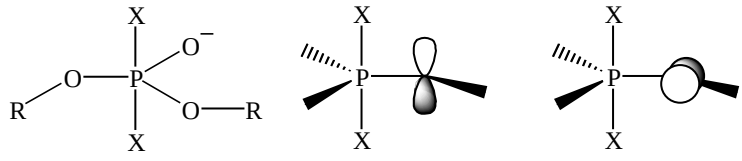

n(||) form n(⊥) form

1 **2** **3**

Williams and co-workers [23, 25*a–d*, *f*, *i*), 27] have provided substantial evidence for concerted processes in transfer reactions of phosphoryl groups between nucleophiles. In the concerted phosphoryl transfer, the reactivity increases when there is a lone pair on the directly attached atom (oxygen in **1**) to the central P, **1**, especially when the p-type lone pair is parallel with the two apical (P—X) bonds of phosphorus, **2**, owing to strong $n_o \rightarrow \sigma^*_{P—X}$ vicinal CT interactions [28]. NBO analyses at the HF/6-311 + G**//B3LYP/6-311 + G** level [28] have shown that for the TBP-5C adduct with R = CH_3 and X = F in **2** the n(⊥) form, **3**, is more stable than the n(||) form, **2**, by $\delta\Delta E = \Delta E(||) - \Delta E(\perp) = 7.3\,\text{kcal mol}^{-1}$. Partition of this energy difference (equation (5)) has led to a greater exclusion repulsion destabilization ($\Delta E_{NCT} > 0$) of $\delta\Delta E$ ($= \Delta E_{NCT}(||) - \Delta E_{NCT}(\perp)) = 15.5\,\text{kcal mol}^{-1}$ for the n(||) form. The CT stabilization ($\Delta E_{CT} < 0$) is also larger for the n(||) than the n(⊥) form, $\delta\Delta E_{CT} = -8.2\,\text{kcal mol}^{-1}$, but the difference is smaller than that for $\delta\Delta E_{NCT}$. Thus, despite the larger CT stabilization with the n(||) than the n(⊥) form, even greater destabilization caused mainly by the exclusion repulsion ($n_o \rightarrow \sigma_{P—X}$ interaction) with the n(||) form results in the overall stability of the n(⊥) relative to the n(||) adduct for X = F. In contrast, the greater stability of n(||) relative to n(⊥) for X = Cl (by $5.2\,\text{kcal mol}^{-1}$) originates from the greater ($n_o \rightarrow \sigma^*_{P—X}$) CT stabilization (by $\delta\Delta E_{CT} = -25.9\,\text{kcal mol}^{-1}$) with smaller repulsive interaction (by $\delta\Delta E_{NCT} = 20.7\,\text{kcal mol}^{-1}$) for the n(||) than the n(⊥) form. Both $n_o \rightarrow \sigma^*_{P—Cl}$ ($-36.2\,\text{kcal mol}^{-1}$) and the overall CT stabilization ($\Delta E_{CT} = -106.7\,\text{kcal mol}^{-1}$) for X = Cl are greater than $n_o \rightarrow \sigma^*_{P—F}$ ($-28.5\,\text{kcal mol}^{-1}$) and the overall CT stabilization ($\Delta E_{CT} = -87.7\,\text{kcal mol}^{-1}$) for X = F in the n(||) forms. The greater $n_o \rightarrow \sigma^*_{P—Cl}$ CT should also mean that bond cleavage of the P—Cl bond is more facilitated than for the P—F bond in the TS. These result from the narrower energy gap $\Delta\varepsilon = \varepsilon_{\sigma^*} - \varepsilon_n$ for X = Cl ($\Delta\varepsilon = 0.2268 - (-0.54714) = 0.7739$ a.u.) than for X = F ($\Delta\varepsilon = 0.6589 - (-0.8215) = 1.4804$ a.u.) in equation (3), which in turn is primarily due to the lower $\sigma^*_{P—Cl}$ than $\sigma^*_{P—F}$ level. Thus, (i) the p lone pair on the atom directly attached to the central P atom exerts an important CT stabilizing effect on the TBP-5C structure, which may be a TS or an intermediate, and (ii) the lower the $\sigma^*_{P—X}$, the greater is the stability of the n(||) form, and hence the greater is the apicophilicity [29] of X. The more apicophilic the leaving group (X = Cl), the lower is the energy, i.e. the greater is the reactivity for the concerted path, as has been shown experimentally [29(*b*)].

4. σ versus π attack processes at unsaturated carbon centres

4.1. *Gas-phase identity nucleophilic substitution of vinyl chloride*

Nucleophilic vinylic substitution can proceed via an intermediate carbanion normally with retention of configuration, or concertedly with concurrent bond formation and cleavage with inversion of configuration [30].

In the former process the adduct, **4**,

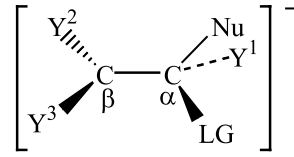

4

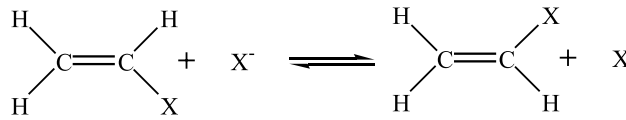

(7)

is a stable intermediate in which the negative charge is delocalized by conjugation in systems activated by electron acceptors at C_β (Y^2 and/or $Y^3 = NO_2$, RCO, RCO_2R, etc.). In the single-step, concerted process **4** is a TS. For unactivated vinylic systems ($Y^1 = Y^2 = Y^3 = H$ in **4**) exclusive inversion in a concerted process (equation (7)) has rarely been observed. However, the vinyl analogue of the aliphatic S_N2 mechanism has been proposed experimentally, mostly for the reactions proceeding with highly S_N1 character [31]. Recently, this type of in-plane S_N2 route with inversion of configuration has been predicted to be theoretically feasible at an unactivated vinylic carbon in the gas phase and in solution [32], (equation (7)). The TS structures for the two types of process, π attack ($S_N\pi$) and σ attack ($S_N\sigma$) S_N2 TSs, determined at the G2(+)MP2 level are shown in figure 2 for X = Cl [5]. The $S_N\pi$ TS is characterized by a tighter bond formation than in the $S_N\sigma$ TS, which is in line with the large short-range effect of proximate $\sigma \rightarrow \sigma^*$ CT stabilization within the $S_N\pi$ TS. It has been shown that, in the intermolecular delocalizations due to the proximate $\sigma \rightarrow \sigma^*$ CT interactions, electron correlation allows the two interacting molecules to approach each other more closely by overcoming a significant amount of exclusion repulsion [13]. The NBO analysis of the TSs has shown that the CT terms, ΔE_{CT}, are much greater for the $S_N\pi$ path at *c.* −557 and −196 kcal mol^{-1} for X = Br and Cl

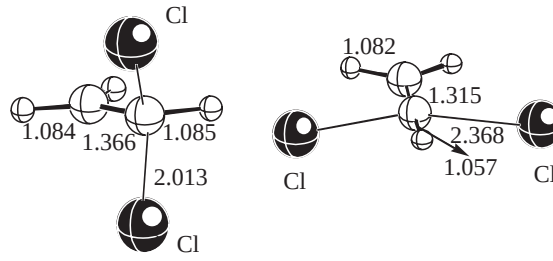

out-of-plane π-attack with retention ($S_N\pi$ TS)

in-plane σ-attack with inversion ($S_N\sigma$ TS)

Figure 2. TS structures with X = Cl at the G2(+)MP2 level.

Table 6. NBO analysis of the $S_N\pi$ and $S_N\sigma$ TSs with X = Cl and Br in the identity gas-phase nucleophilic substitutions at vinyl halides (equation (6)) (energies in kcal mol^{-1}).

Reaction path	X	$\Delta H^{\neq}$ [a] ($\Delta G^{\neq}$)[b]	$-\Delta E_{CT}$	$-\Delta E_{es}$
$S_N\pi$	Cl^-	26.0 (34.5)	196	16
	Br^-	31.8 (39.5)	557	13
$S_N\sigma$	Cl^-	22.8 (29.8)	33	92
	Br^-	25.4 (32.1)	32	73

[a] Enthalpy of activation at G2(+)MP2 level.
[b] Activation free energy at G2(+)MP2 level.

respectively than for the $S_N\sigma$ path at -32 and -33 kcal mol^{-1} for X = Br and Cl respectively (table 6) [5]. In both cases, the $S_N\sigma$ path is energetically favoured over the $S_N\pi$ path with lower barrier heights. This means that the CT stabilization, ΔE_{CT}, is not responsible for the preference of the $S_N\sigma$ over the $S_N\pi$ path, and hence the other component in equation (5), ΔE_{NCT}, should be responsible. Indeed the electrostatic energies are much more stabilizing for the $S_N\sigma$ TS than for the $S_N\pi$ TS. Since the ΔE_{NCT} term also includes exclusion repulsion energy, the preference of the $S_N\sigma$ over the $S_N\pi$ path should also reflect lower repulsion in the looser $S_N\sigma$ TSs than in the more compact $S_N\pi$ TSs.

The NBO analysis clearly demonstrates that the tight $S_N\pi$ TSs are primarily stabilized by the proximate $\sigma \rightarrow \sigma^*$ type CT interactions, whereas the loose $S_N\sigma$ TSs are mainly stabilized by the electrostatic interaction. The electrostatic energies are stronger and more stabilizing in the $S_N\sigma$ TSs than the CT interaction energies in the $S_N\pi$ TSs. The ΔE_{CT} values in the $S_N\pi$ path ($(Br^-(-557$ kcal mol$^{-1}) < Cl^-(-196$ kcal mol$^{-1})$) do not conform to the reactivity pattern ($Cl^-(\Delta G^{\neq} = 30$ kcal mol$^{-1}) < Br^-(32$ kcal mol$^{-1})$ at the G2(+)MP2 level) but the ΔE_{es} values in the $S_N\sigma$ path reflect the correct order ($Cl^-(-92$ kcal mol$^{-1}) < Br^-(-73$ kcal mol$^{-1})$) of reactivity trend [5].

The preferred $S_N\sigma$ over $S_N\pi$ path in the nucleophilic vinyl substitution is in strong contrast to the exclusive $S_N\pi$ reaction path observed in the carbonyl transfers [4(*c*)] (*vide supra*). Structurally the two, carbonyl and vinyl, are related by Y=CHCl where Y = O and CH_2 in the carbonyl and vinyl systems respectively. In other words substitution of Y = O (carbonyl) by CH_2 (vinyl) reverses the identity gas-phase nucleophilic substitution path from an exclusive out-of-plane $S_N\pi$ with retention to an in-plane $S_N\sigma$ with inversion pathway.

In this respect an interesting analysis has been reported on the similar identity S_N2 chloride exchange reaction with Y = NH, i.e. with imidoyl chloride [6].

4.2. *Gas-phase identity nucleophilic substitution of imidoyl chloride*

The NBO analysis of the intrinsic barrier in the chloride exchange of imidoyl chloride

$$HN{=}CHCl + Cl^- \rightleftharpoons Cl^- + HN{=}CHCl, \tag{8}$$

provided an interesting intermediate mechanistic and reactivity behaviour between carbonyl and vinyl carbon substitution. The structures of the three compounds are related by Y = O, HN and CH_2 in Y=CHCl with a decrease in electronegativity, O > N > C. The initial attack of the nucleophile (Cl^-) takes place at the C_α atom

Table 7. Comparisons of activation energies ($\Delta E^{\neq}$)[a], LUMO levels (ε^*) and lobe sizes for the gas-phase identity nucleophilic substitutions of Y═CHCO with Y = O, NH and CH_2.

Compound	LUMO level[b]		Lobe size[b]		$\Delta E^{\neq}$		$\delta\Delta E^{\neq} = \Delta E^{\neq}(\sigma) - \Delta E^{\neq}(\pi)$
	ε_{σ^*}	ε_{π^*}	σ^*	π^*	$S_N\pi$	$S_N\sigma$	
CH_2═CHCl	0.2295	0.2025	0.7448	0.7018	28.3	23.0	−5.3
HN═CHCl	0.1925	0.1002	0.7526	0.7645	6.9	14.9	8.0
O═CHCl	0.1965	0.0795	0.7592	0.8274	−9.2	5.9	15.1

[a] Electronic activation energy, not corrected for ZPEs. Calculated at the G2(+)MP2//MP2/6-311 + G** level in kcal mol^{-1}.
[b] At the RHF/6-311 + + G**//MP2/6-311 + G**level, in a.u.

through highest occupied MO (Cl^-)–LUMO (Y═CHCl) interaction. Thus the $n_{Cl} \rightarrow \pi^*_{Y=CH}$ ($S_N\pi$ path) or $n_{Cl} \rightarrow \sigma^*_{C-Cl}$ ($S_N\sigma$ path) interaction provides a leading term in ΔE_{CT} (equations (3) and (5)). Within the TS, other proximate $\sigma \rightarrow \sigma^*$ CT interactions also contribute to the TS stability. In all cases the $\pi^*_{Y=CH}$ LUMO levels are lower than the σ^*_{C-Cl} levels (table 7), so that the initial attack on the π^* orbital ($S_N\pi$ path) is favoured over that on the corresponding σ^* orbital ($S_N\sigma$ path).

This is not true, however, with $Y = CH_2$ for which the $S_N\sigma$ path is energetically preferred to the $S_N\pi$ path [5]. The $S_N\pi$ routes have lower barriers than $S_N\sigma$ routes for Y = O and NH, although the barriers in general increase in the order $O < NH < CH_2$ [6]. These trends are in accord with the progressive elevation of the LUMOs in the order $O < NH < CH_2$ in table 7. Interestingly the lobe sizes of C_α are greater for the σ^* (0.74 and 0.75 for $Y = CH_2$ and CH_3CH respectively) than for the π^* (0.70 and 0.68 for $Y = CH_2$ and CH_3CH respectively) orbitals with vinyl, which reverses to the larger π^* lobe (0.83 versus 0.76) with carbonyl chlorides, and for the imidoyl chloride the lobe sizes of σ^* and π^* are similar (0.75, 0.76 for σ^* versus 0.76, 0.75 for π^* for Y = NH and CH_3N respectively) [6]. This is in line with the preferred reaction pathway (table 7) for each compound: $S_N\sigma$ for the vinyl, $S_N\pi$ for the carbonyl and the intermediate for the imidoyl chloride.

Examination of TS structures shows that the $S_N\pi$ TSs have relatively tight tetrahedral structure, as we found for the $S_N\pi$ TSs of the vinyl and carbonyl chlorides (figure 3). In contrast, the $S_N\sigma$ TSs are loose with a large degree of C—Cl bond cleavage and small extent of C—Cl bond formation. The natural population analysis (NPA) [13, 33] revealed that the double bond moiety becomes negatively charged in the $S_N\pi$ TSs and positively charged in $S_N\sigma$ TSs. The stability of the $S_N\sigma$ TS depends on that of the cationic moiety $Y \overset{+}{\equiv} CH$, which in turn depends on the σ-accepting power of Y.

The NBO analysis of the proximate $\sigma \rightarrow \sigma^*$ CT interactions (ΔE_{CT}) within the TSs indicated that the relatively tight $S_N\pi$ TSs are stabilized mainly by such CT energies. The reactivity of the $S_N\pi$ path increases in the same order as that for the $S_N\sigma$ path, $Y = CH_2 < NH < O$, but in the former the successive decrease in $\Delta E^{\neq}$ is greater, *c.* 20 kcal mol^{-1}, as Y is varied. Moreover, the absolute proximate $\sigma \rightarrow \sigma^*$ CT stabilization energies are considerably larger in the $S_N\pi$ TS (*c.* −800 and −620 kcal mol^{-1} for Y = NH and CH_2) than in the $S_N\sigma$ TS (*c.* −150 kcal mol^{-1} for both Y = NH and CH_2). Thus the increase in the stability of the $S_N\pi$ TS from $Y = CH_2$ to O is enormous, although the reactivity order is the same as in the $S_N\sigma$

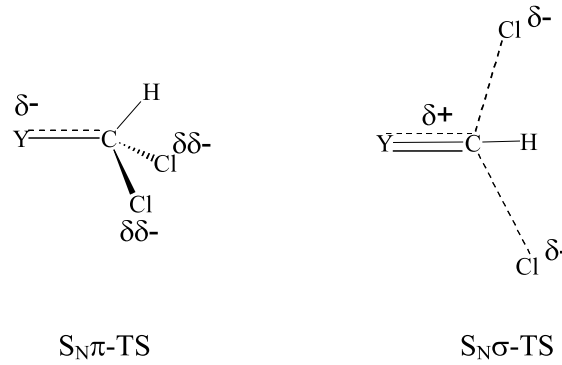

Figure 3. Charge development in the TS.

path. Consequently, the $S_N\pi$ reaction barrier for Y = O is not only much lower (by $\Delta E^{\neq} \cong 38\,\text{kcal mol}^{-1}$) than that for $Y = CH_2$ but also lower (by *c.* $17\,\text{kcal mol}^{-1}$) than the $S_N\sigma$ reaction barrier [6]. This is why the gas-phase chloride exchanges in formyl chloride proceed exclusively by the $S_N\pi$ pathway. However, for the reaction of vinyl chloride, the proximate $\sigma \rightarrow \sigma^*$ CT stabilization in the $S_N\pi$ TS is much smaller (by *c.* $200\,\text{kcal mol}^{-1}$) than that of the imidoyl chloride. This low $\sigma \rightarrow \sigma^*$ CT energy (ΔE_{CT}) for the vinyl chloride in the $S_N\pi$ TS is partly due to the absence of a lone pair, in contrast to the strong $n_Y \rightarrow \sigma^*_{C-Cl}$ CT energies involving the lone pairs on N (imidoyl) and O (formyl). The low ΔE_{CT} value in the $S_N\pi$ TS and relatively strong electrostatic stabilization ($-\Delta E_{es}$ is greater by 40–80 kcal mol^{-1} for the $S_N\sigma$ than the $S_N\pi$ TS for $Y = CH_2$ and NH) in the $S_N\sigma$ TS leads to the preference (by *c* $6\,\text{kcal mol}^{-1}$ at the G2(+) level) for the $S_N\sigma$ path over the $S_N\pi$ path for the vinyl chloride (*vide supra*). Thus, the important factors in favour of the $S_N\sigma$ path over the $S_N\pi$ path for vinyl chloride are (i) weaker CT stabilization (ΔE_{CT}) due to the lack of a lone pair on C (unfavourable for the $S_N\pi$ path), (ii) strong stabilization involving the ΔE_{NCT} term (favourable for the $S_N\sigma$ path) and (iii) the larger lobe size on C_α for the σ^* LUMO than for the π^* LUMO (favourable for $S_N\sigma$ path) [6]. In contrast, for the imidoyl chloride (Y = NH) the energetics for both the $S_N\sigma$ and the $S_N\pi$ paths are intermediate between those of formyl (Y = O) and vinyl ($Y = CH_2$) chloride. In addition, the lobe sizes on C_α are similar in the σ^* and π^* LUMOs. As the electron-donating ability of a substituent in Y increases, the stability of the cationic moiety, $Y \overset{+}{=} CH$, in the $S_N\sigma$ TS increases but that of the anionic $S_N\pi$ TS decreases. This change in the relative stability with a stronger electron donor substituent in Y leads to the greater stability of the $S_N\sigma$ TS but to the lower stability of the $S_N\pi$ TS so that the difference in the two barriers narrows down further as noted for the substituted imidoyl chloride [6].

4.3. *Gas-phase identity nucleophilic substitutions of cyclopropenyl halides*

Nucleophilic substitution at a cyclopropenyl ring carbon atom is of much interest since (i) the displacement can occur by a σ as well as a π attack as presented in figure 4 and (ii) the cyclopropenyl cation and anion that may be involved in the reaction path represent the simplest aromatic (cation with $n = 0$ in the $4n + 2$ aromatic π systems) and antiaromatic (anion with $n = 1$ in the $4n$ antiaromatic π systems)

species respectively. The theoretical results at the G2(+)//MP2/6-311+G** level [7] have indeed shown that the reactivity (F ($\Delta G^{\neq} = 14.3$ kcal mol^{-1}) < Cl (9.1 kcal mol^{-1}) < Br (6.4 kcal mol^{-1})) of σ attack S_N2 reactions of halides (figures 4 and 5) are strongly influenced by the positive charge developed (aromatic character) in the cyclopropenyl ring within the open (loosely bound) TS structure. The NBO analysis revealed that the major stabilizing factor of the σ attack S_N2 TS is a strong CT ($\pi_{C=C} \rightarrow p^+$ interaction) from the $\pi_{C=C}$ orbital to the empty p (p^+) orbital which is left behind after a charge loss to the departing F^- from the ring (figure 5). The $\pi \rightarrow p^+$ CT energy which is the major component of ΔE_{CT} increases successively from −232 (F) to −350 (Cl) and to −378 (Br) kcal mol^{-1} as the ring positive charge (aromatic character) increases from +0.666 (F) to +0.744 (Cl) and to +0.762 (Br). The $n_X \rightarrow p^+$ CT interactions are also conceivable, but they are very weak and insignificant owing to negligible overlap (and hence the matrix element) between the lone pairs on X and p^+ because of the long distance between the two in the $S_N\sigma$ TSs.

The substitution with rearrangement of the double bond through π attack with either the *syn* (S_N2'-*syn*) or the *anti* (S_N2'-*anti*) orientation is powerfully influenced by the proximate CT delocalization of the developing lone pair on C_3 (n_C) toward the two vicinal C—X antibonding (σ^*) orbitals, the two $n_C \rightarrow \sigma^*_{C-X}$ interactions [7] (figure 6). The NBO analyses have shown that in the S_N2'-*syn* adduct (C_s symmetry)

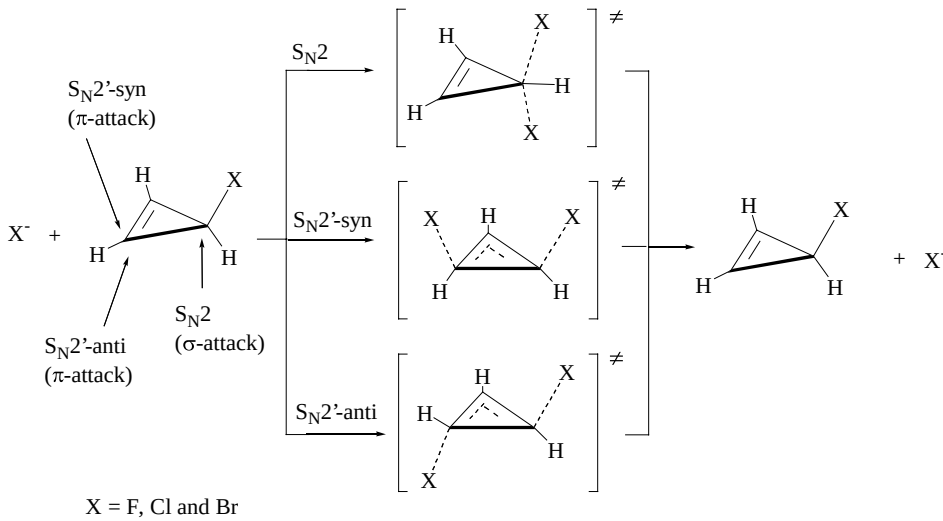

Figure 4. Various reaction paths for the identity nucleophilic substitution in the cyclopropenyl halides.

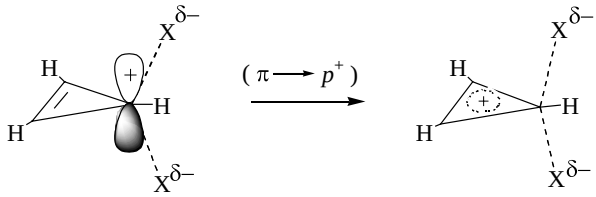

Figure 5. 1,1-Dihalocyclopropenyl-cation-like open TS structure for the σ attack S_N2 processes.

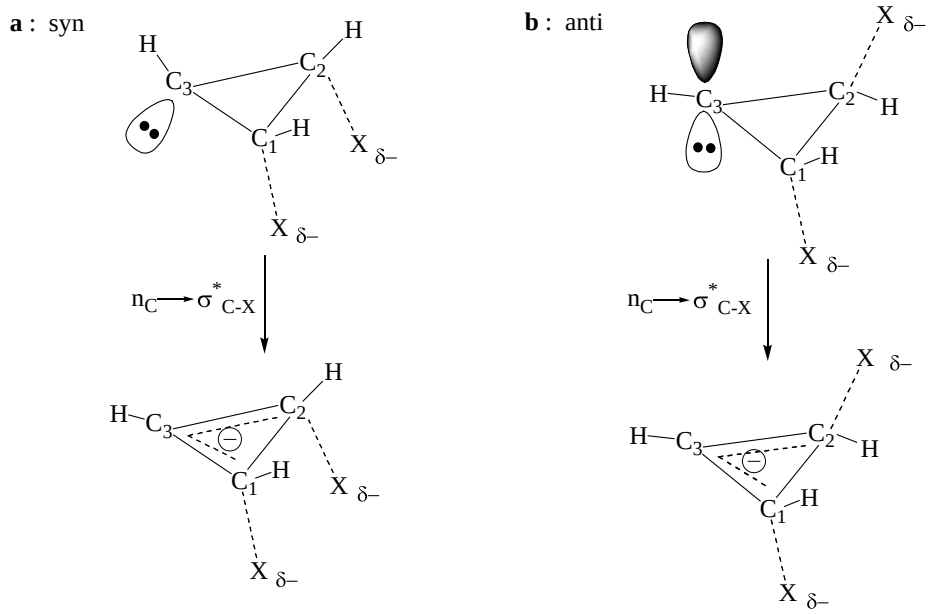

Figure 6. 1,2-Dihalocyclopropyl (delocalized) anion-like TS structures for S_N2' processes.

the lone pair on C_3 is an sp^3 type (lower energy level) and that in the S_N2'-*anti* adduct (C_2 symmetry) is a p type (higher energy level) so that the S_N2'-*anti* TSs are more stabilized owing to greater CT energies (larger $-\Delta E^{(2)}_{\sigma\sigma^*}$ values in equation (3)) than the S_N2'-*syn* TSs. The reaction barriers ($\Delta G^{\neq}$) are −5.6 (F), 7.3 (Cl) and 4.8 (Br) kcal mol^{-1} for the preferred S_N2'-*anti* paths. In contrast, the proximate CT energies (ΔE_{CT}) are −191 (F), −345 (Cl) and −564 (Br) kcal mol^{-1}. Thus the origin of the lowest S_N2' reaction barrier with X = F is not the greater CT stabilization (ΔE_{CT}); on the contrary, ΔE_{CT} is the lowest with X = F. Thus there is again another factor, bond energy of the partially formed C—X bonds within the TS, that is responsible for the greatest reactivity of the S_N2' path for X = F. In fact the two equal C—F bond distances in the S_N2'-*anti* TS are 1.560 Å which are by far shorter (and hence the C—F bonds are much stronger) than the corresponding C—Cl (2.166 Å) and C—Br (2.434 Å) bonds [7]. The S_N2'-*anti* TS with X = F is tighter since the degree of bond formation is approximately 50% for all X (F, 49%; Cl, 54%; Br, 46%), but the extent of bond cleavage is much less for X = F (F, 14%; Cl, 46%; Br, 54%).

Although the S_N2'-*syn* reaction barriers are higher by 5–7 kcal mol^{-1} than for the corresponding S_N2'-*anti* path, the reactivity is again in the order Cl < Br < F and the origin of this reactivity trend is the same as that in the S_N2'-*anti* path. Overall, the barriers are the lowest in the S_N2'-*anti* path and the highest in the S_N2'-*syn* path with the σ attack S_N2 path between.

4.4. *Gas-phase identity nucleophilic substitutions of cyclopentadienyl halides*

The nucleophilic substitution at a cyclopentadienyl carbon provides another interesting reaction that may involve aromatic (anion with $n = 1$ in the $4n + 2$ π system) or antiaromatic (cation with $n = 1$ in the $4n$ π system) species in the reaction path. In addition the reaction presents a variety of reaction pathways as shown in

figure 7. In contrast to the open (loose) TS involved in the identity gas-phase nucleophilic substitution at a cyclopropenyl carbon, the reactions at a cyclopentadienyl carbon have led to rather compact (tight) TS structures in keeping with stabilization through as much aromatic anionic character as possible in the TSs [8]. For example, in the σ attack S_N2 TSs, the two identical C—X bond distances in the C_{2v} structure are shorter than the corresponding C—X bond distances in the saturated reactant, cyclopentyl halides [8]: C—F, (cyclopentadienyl) 1.856 versus (cyclopentyl) 1.894 Å; C—Cl, 2.339 versus 2.414 Å; C—Br, 2.498 versus 2.594 Å. These trends are in strong contrast to the corresponding C—X bond distances in the σ attack S_N2 TSs for cyclopropenyl halide exchanges where the C—X bonds are longer than those for the saturated, cyclopropyl, halides [7]: C—F, (cyclopropenyl) 2.069 versus (cyclopropyl) 1.852 Å; C—Cl, 2.681 versus 2.349 Å; C—Br, 2.873 versus 2.517 Å. NPA showed that the charges at the C_1 atom in the $S_N\sigma$ TS are $q_1^{\neq} = 0.149$ (X = F), −0.112 (Cl) and −0.159 (Br). These results clearly show that the $S_N\sigma$ path of fluoride is unfavourable ($\delta\Delta G^{\neq} = \Delta G^{\neq}(S_N\sigma) - \Delta G^{\neq}(\text{s-}S_N\sigma) = +1.5\,\text{kcal mol}^{-1}$) whereas those of chloride and bromide are favourable ($\delta\Delta G^{\neq} = -1.6$ and $-2.8\,\text{kcal mol}^{-1}$ for X = Cl and Br respectively) over the corresponding reactions with cyclopentyl halides (s-$S_N\sigma$) owing to antiaromatic cationic charge (X = F) and aromatic anionic charge (X = Cl and Br) development in the TSs.

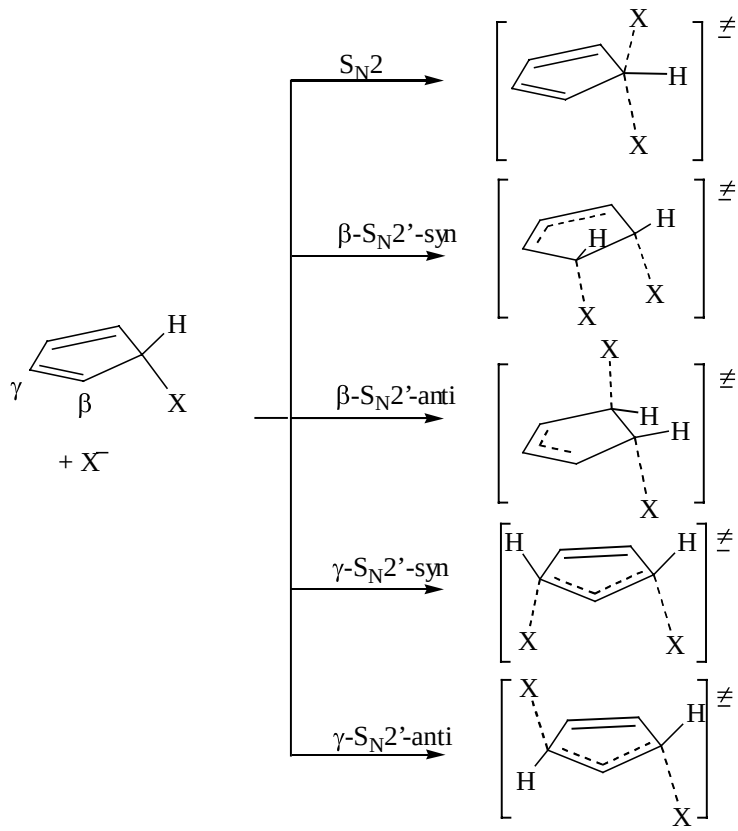

Figure 7. Various reaction pathways for the identity nucleophilic substitution reactions in cyclopentadienyl halides.

In the TBP-5C TS (similar to that shown in figure 5 for the cyclopropenyl halides) an empty p orbital develops as the leaving group, X^-, departs, and leads to strong electronic charge delocalization from the lone pair orbitals on both X atoms toward the empty p (p^+) orbital on C_1 ($n_X \rightarrow p^+$ CT interactions) and the TS is stabilized as much as possible by preventing the formation of an antiaromatic cyclopentadienyl cationic ring structure. In this respect, NBO analysis reveals interesting aspects of the proximate $\sigma \rightarrow \sigma^*$ CT interactions in the $S_N\sigma$ TSs. The results are presented in table 8 where two types of major CT interactions, $\pi_{C=C} \rightarrow p^+$ and $n_X \rightarrow p^+$, are analysed. The lone pair orbital on halide (n_X) is also a p type. We note that although the lone pair on X (n_X) is farther away from the p^+ orbital than the $\pi_{C=C}$ orbital, the overlap (represented by F_{ij} which is proportional to the overlap integral) is greater and as a result the CT energy is much greater. This is because the p^+ orbital in the $\pi_{C=C} \rightarrow p^+$ interaction overlaps sideways with only a nearest carbon atom of the C=C π bond. Thus in the $S_N\sigma$ TS of the nucleophilic substitution of cyclopentadienyl halide, the $n_X \rightarrow p^+$ interaction provides the major stabilizing effect, and the $\pi_{C=C} \rightarrow p^+$ interaction is only a minor stabilizing factor. This is quite the opposite situation to that found in the nucleophilic substitution at a cyclopropenyl halide, where the $\pi_{C=C} \rightarrow p^+$ interaction was found to provide the major stabilization effect in the $S_N\sigma$ TSs [7]. This is due to the close distance between $\pi_{C=C}$ and p^+ with the overlap of both carbon atoms in the $\pi_{C=C}$ orbital in the cyclopropenyl case, where of course the $n_X \rightarrow p^+$ interaction is much weaker owing to long distance between the X and p^+ centres.

As to the $S_N\sigma$ reactivity order for the cyclopentadienyl halides Cl ($\Delta G^{\neq} = 10.1\,\text{kcal mol}^{-1}$) < Br ($8.9\,\text{kcal mol}^{-1}$) < F ($8.5\,\text{kcal mol}^{-1}$), the bond energy and exclusion repulsion effects included in the NCT (ΔE_{NCT}) term are stronger than

Table 8. NBO analyses of two major CT interactions in the $S_N\sigma$ pathways involved in the identity nucleophilic substitutions of cyclopentadienyl halides.

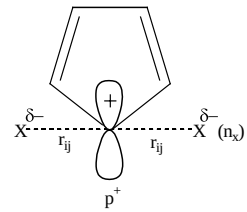

	$\pi_{C=C} \rightarrow p^+$			$n_X \rightarrow p^+$		
X	F	Cl	Br	F	Cl	Br
$r_{ij}^{\neq a}$	1.490	1.480	1.478	1.856	2.339	2.498
$\Delta\varepsilon_{ij}{}^b$	0.43	0.32	0.30	0.67	0.34	0.28
$F_{ij}{}^c$	0.103	0.109	0.112	0.296	0.220	0.198
$-\Delta E_{ij}^{(2)\,d}$	25.1	33.9	37.1	147.3	154.7	149.3

[a] Distance (Å) between the two interacting orbitals. For $\pi_{C=C}$, the carbon atom nearest to the p^+ is taken.
[b] The energy gap (a.u.), $\Delta\varepsilon_{ij} = \varepsilon_{p+} - \varepsilon_{nx}$ (or $\varepsilon_{C=C}$).
[c] Fock matrix element in a.u.
[d] CT energy in kcal mol^{-1}.

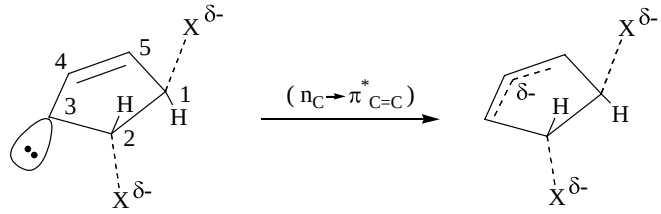

Figure 8. β–S_N2'-*anti* TS.

the CT stabilization (ΔE_{CT}), which differs little between the halides (X). The NBO analysis of the π attack β-S_N2' paths shows that in both the *syn* (C_s symmetry) and the *anti* (C_1 symmetry) TSs an incipient lone pair formed on C_3 (sp^3 type in the *syn* and p type in the *anti* path) is delocalized toward the C═C bond by a strong $n_C \rightarrow \pi^*_{C=C}$ CT interaction and a delocalized allyl anionic structure is formed over the C_3—C_4—C_5 moiety as shown in figure 8. There are also weak vicinal $n_C \rightarrow \sigma^*_{C-X}$ interactions in all of the β-S_N2' TSs. The overall CT energies (ΔE_{CT}) are stronger in the *anti* TSs than the *syn* TSs, which leads to lower activation energies for the β-S_N2' *anti* paths. For the β-S_N2' paths also the fluoride exchanges have a considerably lower barrier despite the similar proximate CT stabilizations, e.g. for the *anti* path $\Delta G^{\neq} = -1.0$ (F), 20.2 (Cl) and 18.6 (Br) kcal mol^{-1}. The major contribution to this low barrier for X = F again comes from the strong bond energy of the two partially formed C—F bonds in the TS. The C—F bonds in the TS are much tighter (and hence the bonds are stronger) than the corresponding C—Cl and C—Br bonds, with much lower extent of bond cleavage: F, 6%; Cl, 29%; Br, 47%.

The nucleophile can substitute at a γ-carbon leading to either a *syn* (γ-S_N2'-*syn*) or an *anti* (γ-S_N2'-*anti*) orientation to the C—X bond in the TS. A lone pair develops at the β-(C_2) carbon in the γ-S_N2', a p type for the *anti* and an sp^3 type for the *syn* (figure 9), and relatively strong $n_C \rightarrow \sigma^*_{C-X}$ vicinal CT occurs and the C_1—C_2—C_3 moiety becomes a delocalized allyl anion. There are also very weak $\pi_{C=C} \rightarrow \sigma^*_{C-X}$ CT interactions. The $\Delta E^{(2)}_{\pi\rightarrow\sigma^*}$ values range from −8 (X = F) to −16 (X = Br) kcal mol^{-1} whereas the $\Delta E^{(2)}_{n\rightarrow\sigma^*}$ values are much larger than these, ranging from −67 (X = F) to −219 (X = Br) kcal mol^{-1}. The latter $\Delta E^{(2)}_{n\rightarrow\sigma^*}$ CT energies in the γ-S_N2' TSs are, however, considerably lower than the $n_C \rightarrow \sigma^*_{C=C}$ interaction energies (−198 to −334 kcal mol^{-1}) in the β-S_N2' TSs (figure 8) mainly because of wider energy gaps ($\Delta\varepsilon = \varepsilon_{\sigma^*} - \varepsilon_n$ in equation (3)) with the lower n levels (e.g. $\varepsilon_n = 0.022$ (*syn*) and 0.019 (*anti*) a.u in the γ-S_N2' TSs versus $\varepsilon_n = 0.025$ (*syn*) and 0.026 (*anti*) a.u. in the β-S_N2' TSs for X = Cl] and the higher σ^*_{C-X} than $\pi^*_{C=C}$ levels. Delocalization of the lone pairs on C_2 in the γ-S_N2' TSs is less (or more localized) than of those on C_4 in the β-S_N2' TSs.

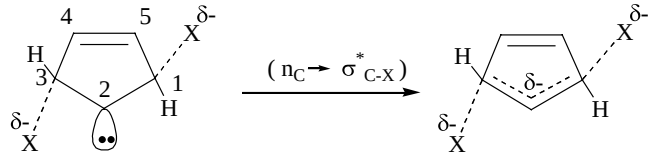

Figure 9. γ–S_N2' *anti* TS.

The proximate CT stabilization (ΔE_{CT}) of the γ-S_N2' TS increases in the order X = F < Cl < Br, which does not conform to the barrier height decrease: Cl ($\Delta G^{\neq} \cong 19\,kcal\,mol^{-1}$) > Br ($17\,kcal\,mol^{-1}$) > F ($3$–$5\,kcal\,mol^{-1}$). Thus X = F has the lowest proximate CT TS stability but has the highest reactivity. This trend is similar to that found in the β-S_N2' processes and can be associated with the stronger gain of the C—F bond energy relative to C—Cl and C—Br bonds in the β-S_N2' as well as γ-S_N2' TSs.

Although the differences in the $\Delta G^{\neq}$ values between γ-S_N2'-*syn* and -*anti* processes are almost insignificant for X = Cl and Br, there is *c.* $2\,kcal\,mol^{-1}$ difference in favour of *syn* for X = F. This appears to be caused by the stronger $n_C \rightarrow \sigma^*_{C-F}$ interaction in the *syn* ($-68.8\,kcal\,mol^{-1}$) than *anti* ($-66.7\,kcal\,mol^{-1}$) processes leading to stronger delocalized allyl anionic moiety (C_1—C_2—C_3) as evidenced by the lower negative charge on C_2 for *syn* (-0.609) than *anti* (-0.619).

5. Concluding remarks

In this review applications of the NBO method to analysis of the intrinsic reaction barriers involved in the identity nucleophilic substitution of halides (X = F, Cl, Br) at various saturated and unsaturated carbon centres have been surveyed.

These NBO analyses revealed that the stabilization provided by the proximate (geminal and vicinal) $\sigma \rightarrow \sigma^*$ CT interactions in the TS is crucial in determining most of the intrinsic reaction barriers, especially for those involved in the π attack processes. In addition, the electrostatic interaction has emerged as an important factor conducive to the energetic preference for the in-plane σ attack S_N2 pathway. The changes in NBO parameters associated with activation processes also allow a detailed picture of a specific $\sigma \rightarrow \sigma^*$ interaction, which in turn enables one to comprehend and conceptualize the origins of the intrinsic reaction barriers in terms of orbital interactions. The general success of NBO analysis in treating intrinsic reaction barriers provided evidence for the usefulness of the method in conceptualizing the reactivity pattern and for the important role of $\sigma \rightarrow \sigma^*$ CT interaction in understanding the origins of the intrinsic reaction barriers. The NBO analysis presented in this review has been focused on intrinsic reaction barriers involved in the nucleophilic substitution reactions, but applications can readily be extended to analysis of the origins of other types of reaction barriers [14(*b*), 28, 34], as it has been extended to various types of *intra*molecular phenomena such as rotational barriers [13, 35], the anomeric effect [36], conformational stabilities [13, 37] etc.

Acknowledgements

The author thanks Inha University for the continued support for the series of his work reviewed here. He also acknowledges with gratitude the contributions of many co-workers, as cited in the references.

References

[1] (*a*) Shaik, S. S., Schlegel, H. B., and Wolfe, S., 1992, *Theoretical Aspects of Physical Organic Chemistry. The S_N2 Mechanism* (New York: Wiley); (*b*) Keil, F., and Ahlrichs, R., 1976, *J. Am. Chem. Soc.*, **98**, 4787; (*c*) Sini, G., Shaik, S. S., Lefour, J. M., Ohanessian, G., and Hiberty, P. C., 1989, *J. phys. Chem.*, **93**, 5661; (*d*) Vetter, R., and Zülicke, L., 1990, *J. Am. Chem. Soc.*, **112**, 5136; (*e*) Shi, Z., and Boyd, R.,

1990, *J. Am. Chem. Soc.*, **112**, 6789; (*f*) Deng, L., Branchadell, V., and Ziegler, T., 1994, *J. Am. Chem. Soc.*, **116**, 10645; (*g*) Lee, I., Kim, C. K., Chung, D. S., and Lee, B.-S., 1994, *J. org. Chem.*, **59**, 4490; (*h*) Park, Y. S., Kim, C. K., Lee, B.-S., and Lee, I., 1995, *J. org. Chem.*, **99**, 1310; (*i*) Glukhovtsev, M. N., Pross, A., and Radom, L., 1995, *J. Am. Chem. Soc.*, **117**, 2024; (*j*) Uggerud, E., 1999, *J. Chem. Soc. Perkin Trans. 2*, 1459; (*k*) Botschwina, P., 1998, *Theor. Chem. Acc.*, **99**, 426; (*l*) Parthiban, S., De Oliveira, G., and Martin, J. M. L., 2001, *J. phys. Chem.* A, **105**, 895; (*m*) Wladkowski, B. D., Allen, W. O., and Brauman, J. I., 1994, *J. phys. Chem.*, **98**, 13532; (*n*) Lee, I., Kim, C. K., Sohn, C. K., Li, H. G., and Lee, H. W., 2001, *J. phys. Chem.*, **106**, 108.

[2] (*a*) Vande Linde, S. R., and Hase, W. L., 1990, *J. chem. Phys.*, **93**, 7962; (*b*) Cho, Y. J., Vande Linde, S. R., Zhu, L., and Hase, W. L., 1992, *J. chem. Phys.*, **96**, 8275; (*c*) Hase, W. L., and Cho, Y. J., 1993, *J. chem. Phys.*, **98**, 8626; (*d*) Li, G., and Hase, W. L., 1999, *J. Am. Chem. Soc.*, **121**, 7124; (*e*) Vande Linde, S. R., and Hase, W. L., 1990, *J. phys. Chem.*, **94**, 2778; (*f*) Tucker, S. C., and Truhlar, D. G., 1990, *J. Am. Chem. Soc.*, **112**, 3338; (*g*) Clay, D. C., and Palma, J., 1997, *J. chem. Phys.*, **106**, 575; (*h*) Hernandez, M. I., Campos-Martinez, J., Villarreal, P., Schmatz, S., and Clary, D. C., 1999, *Phys. Chem. chem. Phys.*, **1**, 1197.

[3] (*a*) Pellerite, M. J., and Brauman, J. I., 1983, *J. Am. Chem. Soc.*, **105**, 2672; (*b*) Barlow, S. E., van Doren, J. M., and Bierbaum, V. M., 1988, *J. Am. Chem. Soc.*, **110**, 7240; (*c*) van Doren, J. M., Depuy, C. H., and Bierbaum, V. M., 1989, *J. phys. Chem.*, **93**, 1130; (*d*) Depuy, C. H., Gronert, S., Mullin, A., and Bierbaum, V. M., 1990, *J. Am. Chem. Soc.*, **112**, 8650; (*e*) Wilbur, J. L., Wladkowski, B. D., and Brauman, J. I., 1993, *J. Am. Chem. Soc.*, **115**, 10823; (*f*) Wladkowski, B. D., and Brauman, J. I., 1993, *J. phys. Chem.*, **97**, 13158; (*g*) Li, C., Ross, P., Szulejko, J. E., and McMahon, T. B., 1996, *J. Am. Chem. Soc.*, **118**, 9360; (*h*) de Turi, V. F., Hintz, P. A., and Ervin, K. N., 1997, *J. phys. Chem.* A, **101**, 5969; (*i*) Craig, S. L., and Brauman, J. I., 1999, *J. Am. Chem. Soc.*, **121**, 6690; (*j*) Tonner, D. S., and McMahon, T. B., 2000, *J. Am. Chem. Soc.*, **122**, 8783; (*k*) Pellerite, M. J., and Brauman, J. I., 1980, *J. Am. Chem. Soc.*, **102**, 5993.

[4] (*a*) Lee, I., Lee, D., and Kim, C. K., 1997, *J. phys. Chem.* A, **101**, 879; (*b*) Kim, C. K., Li, H. G., Lee, H. W., Sohn, C. K., Chun, Y. I., and Lee, I., 2000, *J. phys. Chem.* A, **104**, 4069; (*c*) Lee, I., Kim, C. K., Li, H. G., Sohn, C. K., Kim, C. K., Lee, H. W., and Lee, B.-S., 2000, *J. Am. Chem. Soc.*, **122**, 11162.

[5] Kim, C. K., Hyun, K. H., Kim, C. K., and Lee, I., 2000, *J. Am. Chem. Soc.*, **122**, 2294.

[6] Li, H. G., Kim, C. K., Lee, B.-S., Kim, C. K., Rhee, S. K., and Lee, I., 2001, *J. Am. Chem. Soc.*, **123**, 2326.

[7] Kim, C. K., Li, H. K., Lee, B.-S., Kim, C. K., Lee, H. W., and Lee, I., 2002, *J. org. Chem.*, **67**, 1953.

[8] Lee, I., Li, H. G., Kim, C. K., Lee, B.-S., Kim, C. K., and Lee, H. W., *Bull. Korean Chem. Soc.* (in press).

[9] Asubiojo, O. I., and Brauman, J. I., 1979, *J. Am. Chem. Soc.*, **101**, 3175.

[10] Wladkowski, B. D., Wilbur, J. L., and Brauman, J. I., 1994, *J. Am. Chem. Soc.*, **116**, 2471.

[11] Zhong, M., and Brauman, J. I., 1999, *J. Am. Chem. Soc.*, **121**, 2508.

[12] Brunck, T. K., and Weinhold, F., 1979, *J. Am. Chem. Soc.*, **101**, 1700.

[13] Reed, A. E., Curtiss, L. A., and Weinhold, F., 1988, *Chem. Rev.*, **88**, 899.

[14] (*a*) Glendening, E. D., and Weinhold, F., 1998, *J. comput. Chem.*, **19**, 593; (*b*) Glendening, E. D., Badenhoop, J. K., and Weinhold, F., 1998, *J. comput. Chem.*, **19**, 628.

[15] Pross, A., and Shaik, S. S., 1983, *Acc. chem. Res.*, **16**, 363.

[16] Wolfe, S., Mitchell, D. J., and Schlegel, H. B., 1981, *J. Am. Chem. Soc.*, **103**, 7694.

[17] Epiotis, N. D., Cherry, W. R., Shaik, S. S., Yates, R., and Bernardi, F., 1977, *Structural Theory of Organic Chemistry* (Berlin: Springer).

[18] Reed, A. E., and Weinhold, F., 1983, *J. chem. Phys.*, **78**, 4066.

[19] Mitchell, D. J., 1981, PhD thesis, Queen's University, Ontario, Canada.

[20] KLUMPP, G. W., 1982, *Reactivity in Organic Chemistry* (New York: Wiley), p. 38.
[21] MITCHELL, D. J., SCHLEGEL, H. B., SHAIK, S. S., and WOLFE, S., 1985, *Can. J. Chem.*, **63**, 1642.
[22] (*a*) HOUK, K. N., GUSTABSON, S. M., and BLACK, K., 1992, *J. Am. Chem. Soc.*, **114**, 8565; (*b*) LEE, I., KIM, C. K., and LEE, B.-S., 1995, *J. comput. Chem.*, **16**, 1045; (*c*) LEE, J. K., KIM. C. K., and LEE, I., 1997, *J. phys. Chem.* A, **101**, 2893.
[23] WILLIAMS, A., 2000, *Concerted Organic and Bio-organic Mechanisms* (Boca Raton, FL: CRC Press).
[24] YAMABE, S., and MINATO, T., 1983, *J. org. Chem.*, **48**, 2972.
[25] (*a*) BA-SAIF, S. A., WARING, M. A., and WILLIAMS, A., 1990, *J. Am. Chem. Soc.*, **112**, 8115; (*b*) BOURNE, N., CHRISTIUK, E., DAVIS, A. M., and WILLIAMS, A., 1988, *J. Am. Chem. Soc.*, **110**, 1890; (*c*) DOUGLAS, K. T., and WILLIAMS, A., 1976, *J. chem. Soc. Perkin Trans. 2*, 515; (*d*) HALL, C. R., and INCH, T. D., 1980, *Tetrahedron*, **26**, 2059; (*e*) HUDSON, R. F., and GREEN, M., 1963, *Angew. Chem. int. Edn. Engl.*, **2**, 11; (*f*) BA-SAIF, S. A., WARING, M. A., and WILLIAMS, A., 1991, *J. Chem. Soc. Perkin Trans. 2*, 1653; (*g*) WILLIAMS, A., 1985, *J. Am. Chem. Soc.*, **107**, 6335; (*h*) BOURNE, N., and WILLIAMS, A., 1984, *J. Am. Chem. Soc.*, **106**, 7591; (*i*) WARING, M. A., and WILLIAMS, A., 1989, *J. Chem. Soc. chem. Commun.*, 1742.
[26] (*a*) WESTHEIMER, F. H., 1968, *Acc. chem. Res.*, **1**, 70; (*b*) COOK, R. D., DIEBER, C. E., SCHWARZ, W. J., TURLEY, P. C., and HAAKE, P., 1973, *J. Am. Chem. Soc.*, **95**, 8088; (*c*) TRIPPETT, S., 1974, *Pure Appl. Chem.*, **40**, 595.
[27] (*a*) WILLIAMS, A., 1994, *Chem. Soc. Rev.*, **23**, 93; (*b*) Page, M. I., and WILLIAMS, A., 1997, *Organic and Bio-organic Mechanisms* (Harlow: Longman).
[28] LEE, H. W., GUHA, A. K., KIM, C. K., and LEE, I., 2002, *J. org. Chem.*, **67**, 2215.
[29] (*a*) MCDOWELL, R. S., and STREITWIESER, A., 1985, *J. Am. Chem. Soc.*, **107**, 5849; (*b*) ROWELL, R., and GORENSTEIN, D. G., 1981, *J. Am. Chem. Soc.*, **103**, 5894.
[30] (*a*) RAPPOPORT, Z., 1969, *Adv. phys. org. Chem.*, **7**, 1; (*b*) MODENA, C. T., 1971, *Acc. chem. Res.*, **4**, 73; (*c*) APELOIG, Y., and RAPPOPORT, Z., 1979, *J. Am. Chem. Soc.*, **101**, 5095; (*d*) RAPPOPORT, Z., 1981, *Acc. chem. Res.*, **14**, 7.
[31] (*a*) CLARK, T. C., KELSEY, D. R., and BERGMAN, R. G., 1972, *J. Am. Chem. Soc.*, **94**, 3626; (*b*) SUMMERVILLE, R. H., SENKLER, C. A., SCHLEYER, P. V. R., DUEBER, T. E., and STANG, P. J., 1974, *J. Am. Chem. Soc.*, **96**, 1100; (*c*) OKUYAMA, T., and OCHIAI, M., 1997, *J. Am. Chem. Soc.*, **119**, 4785; (*d*) OCHIAI, M., OSHIMA, K., and MASAKI, Y., 1991, *J. Am. Chem. Soc.*, **113**, 7059; (*e*) LUCCHINI, V., MODENA, G., and PASQUATO, L., 1993, *J. Am. Chem. Soc.*, **115**, 7059.
[32] GLUKHOVTZEV, M. N., PROSS, A., and RADOM, L., 1994, *J. Am. Chem. Soc.*, **116**, 5961.
[33] REED, A. E., WEINSTOCK, R. B., and WEINHOLD, F., 1985, *J. chem. Phys.*, **83**, 735.
[34] (*a*) MUSSO, G. F., FIGARI, G., and MAGNASCO, V., 1985, *J. Chem. Soc. Faraday Trans., 2*, **81**, 1243; (*b*) PARK, Y. S., KIM, W. K., KIM, Y. B., and LEE, I., 2000, *J. org. Chem.*, **65**, 3997.
[35] (*a*) TYRRELL, J., WEINSTOCK, R. B., and WEINHOLD, F., 1981, *Int. J. quantum Chem.*, **19**, 781; (*b*) POPHRISTIC, V., GOODMAN, L., and GUCHHAIT, N., 1997, *J. phys. Chem.* A, **101**, 4290.
[36] CARBALLEIRA, L., and PEREZ-JUSTE, I., 2000, *J. phys. Chem.* A, **104**, 9362.
[37] (*a*) MATTMANN, E., MATHEY, F., SEVIN, A., and FRISON, G., 2002, *J. org. Chem.*, **67**, 1208; (*b*) SICILIA, E., and RUSSO, N., 2002, *J. Am. Chem. Soc.*, **124**, 1471; (*c*) WANG, P., ZHANG, Y., GLASER, R., REED, A. E., SCHLEYER, P. v. R., and STREITWIESER, A., 1991, *J. Am. Chem. Soc.*, **113**, 55.